Site-characterization update for the seismic array SSCN

Author: A. Imtiaz
Verification team: A. Imtiaz, P. Bergamo, D. Chieppa, D. Fäh
Date: Report SED, 09.01.2024

Introduction:

This report provides an update of the site-characterization for the seismic array site SSCN. We apply a novel Bayesian inversion approach based on a Multizonal Transdimensional Inversion (MTI), developed by Hallo et al. (2021), to retrieve one-dimensional (1D) shear-wave velocity (Vs) profiles with associated uncertainties.

Method:

The MTI is based on a joint inversion of multimodal Rayleigh- and Love-wave dispersion curves (DCs) along with Rayleigh-wave ellipticity. The number of layers in the inversion is determined self-adaptively from the measured data, and model uncertainties are assessed quantitatively. The solution of the Bayesian inversion is presented as the posterior Probability Density Function (PDF) that results from the prior expectations and the observed data supplemented by an expected distribution of data errors. Two options could be considered for the parameterization of the model space: 1) a single-zone transdimensional model space with homogeneous prior assumptions on models, or 2) a multizonal model space with additional constraints on the depths of intermediate layers.

The output from MTI is presented as an ensemble of layered velocity models that represents a discrete approximation of the posterior PDF. It is used for evaluating marginal histograms of subsurface properties such as P-wave velocity (Vp), S-wave velocity (Vs), density (ρ), Poisson's ratio (ν) along the depth. The distribution of MTI results is presented by:

- MAX of PDF: The marginal posterior maximum profile (MAX of PDF) profile, determined by the most frequent value of a property (Vs, Vp, ρ) at each discrete depth across the ensemble of solutions.
- AM of PDF: The marginal posterior average profile (AM of PDF) and its uncertainty (AM$\pm\sigma$), determined by taking the arithmetic mean and the standard deviation of a property (1/Vs, 1/Vp, ρ) at each discrete depth across the ensemble of solutions.

Single representative 1D models of the properties can also be retrieved from the MTI results. However, it is important to keep in mind that the solution of the Bayesian inversion is the whole posterior PDF. Following single 1D models are retrieved:

- ML model: The maximum likelihood (ML) model, defined as the model with the lowest misfit between the observed and modeled data.
- MAP model: The maximum a posteriori (MAP) model, estimated by minimizing the misfit between the MAX of PDF of the velocity and the ensemble of models.

Site and Inputs:

The ambient vibration array SSCN is located at the Novartis industrial complex in Muttenz area in the canton of Basel-Landschaft (BL). The permanent station SSCN (replacement for the station SCHC) belonging to the Swiss Strong Motion Network (SSMNet, Phase II; Hobiger et al., 2021), is located nearby and operating since 2014. Ambient vibration array measurement was performed at the site SBIF in 2016 and a set of 'best' Vs profiles were obtained by Michel et al. (2016).

For the MTI inversion, the processed (Michel et al., 2016) fundamental modes of Rayleigh and Love wave, and the first mode of Rayleigh wave DCs have been used. The ellipticity has been calculated from the central station (SCN000) of the array by using the RayDec (Hobiger et al., 2009) algorithm. Inversions using both single-zone and multizonal model spaces have been performed, and the best fit was achieved from the latter.

Results:

Results of the MTI inversion are shown in the figures below. Figure 1 shows the fit between the DCs from real and model data. The left panels of Figure 2 and Figure 3 show the velocity profiles in terms of posterior marginal PDF of Vs and Vp, respectively, overlaid by the ML and MAP models. The model parameters are well resolved up to the depth where a relatively narrow posterior PDF with very high probability values are observed. The histogram of layer interfaces along the depth of the profile is presented in the right panel of Figure 2 and Figure 3. It shows the probable presence of different primary interfaces at different depths, sharper interfaces indicating lower uncertainties.

The quarter-wavelength (QWL) velocity (Joyner et al., 1981) from the models are calculated. It provides, for a given frequency, the average velocity at a depth corresponding to one-quarter of the wavelength of interest. The QWL parameters are presented in the top panel of Figure 4. The QWL impedance-contrast introduced by Poggi et al. (2012) corresponds to the ratio between two QWL average velocities, respectively from the top and the bottom part of the velocity profile, at a given frequency. The inverse of this impedance shows peaks at resonance frequencies, which could be associated with the QWL depths and velocities. The distribution of Vs_{30} (the time-averaged Vs up to 30 m depth) computed from the inverted models and the corresponding QWL frequencies are shown in the bottom panel of the Figure 4.

The theoretical SH-wave transfer functions (SHTFs) are computed from the inverted models and are compared with the empirical amplification function (EAF) obtained from the earthquakes recorded by the seismic station SSCN by using the empirical spectral modeling (ESM; Edwards et al., 2013). Both are corrected with respect to the Swiss reference rock model (Poggi et al., 2011). The unreferenced SHTFs, and referenced SHTFs and EAF are shown in the left and right panels, respectively, of the Figure 5.

Although the result of the Bayesian inversion is the posterior PDF, a single representative 1D model is usually required for further analysis. Among the velocity profiles retrieved from MTI results, the ML model provides the lowest data misfit, the MAP model is the most probable,

MAX of PDF is a profile of the most frequent values in the ensemble of solutions, and AM of PDF is a profile of average values of the ensemble of solutions (preserving traveltime of a vertically propagating wave). As the MAP model is the most representative in terms of the posterior PDF of Vs, it is recommended to use it as a reference solution. Therefore, Vs_{30} of the MAP model (551 m/s) has been used here to assign the soil classe B according to both SIA 261 (2020) and Eurocode 8 (2004) building codes.
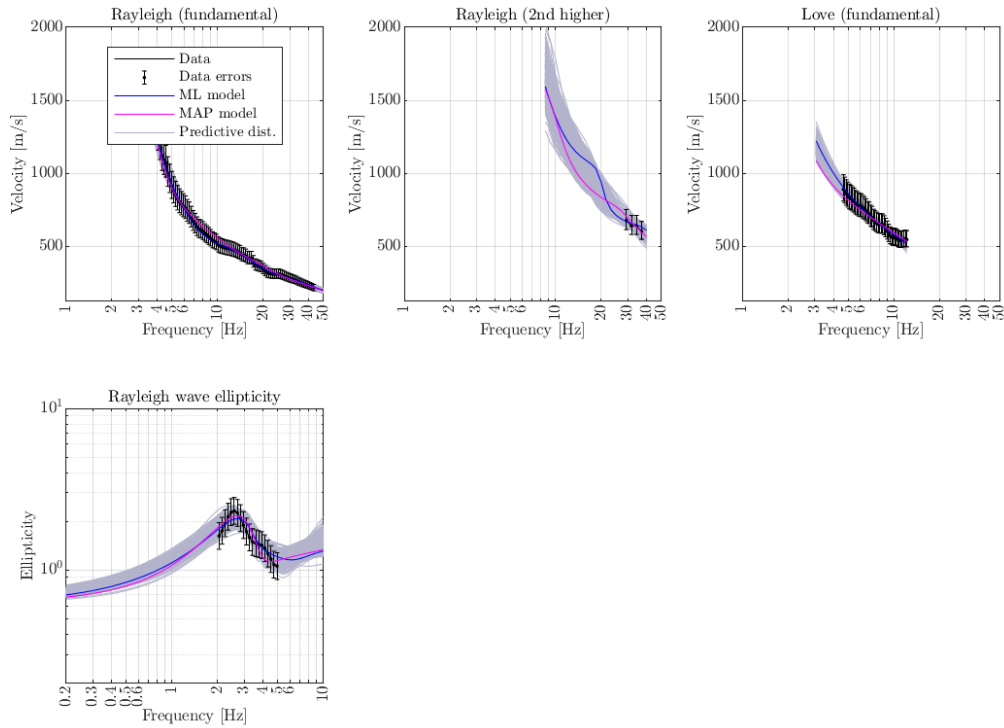
Figure 1: Fit of DCs between the real and modeled data. The real data measured at the site with their uncertainty bounds are shown in black curves with error bars. The modeled data from the inversion are represented as the posterior predictive distribution (grey), ML model (blue), and MAP model (magenta).
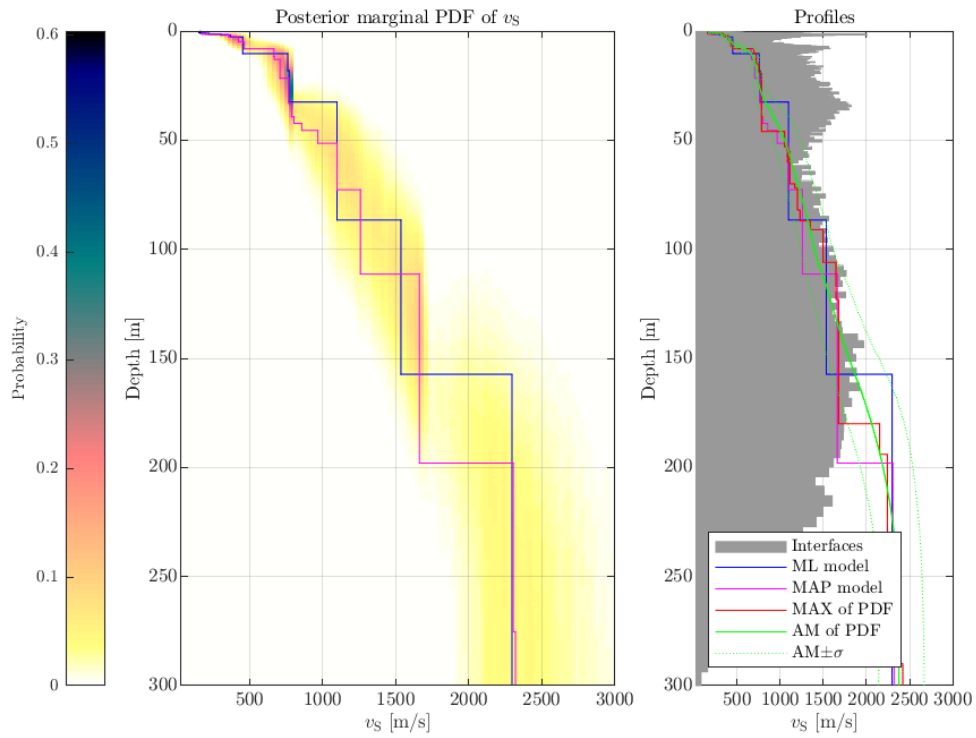
Figure 2: (Left) Posterior marginal PDF (color bar) of the Vs overlaid by the retrieved ML and MAP models. (Right) Histogram of the layer interfaces overlaid by the retrieved models.
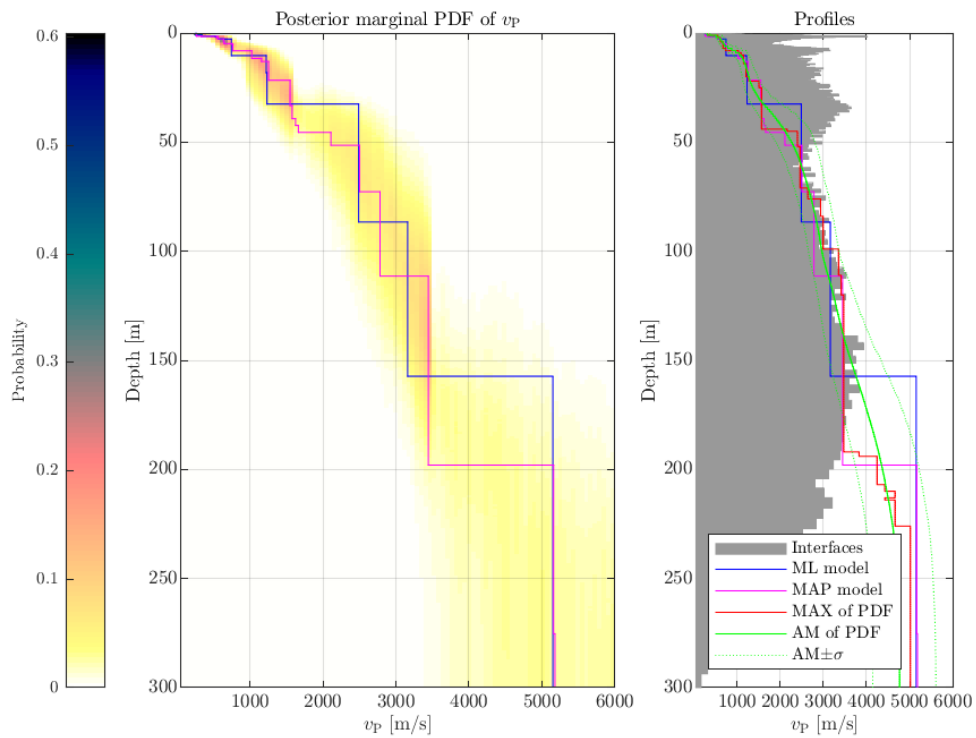

Figure 3: (Left) Posterior marginal PDF (color bar) of the Vp overlaid by the retrieved ML and MAP models. (Right) Histogram of the layer interfaces overlaid by the retrieved models.
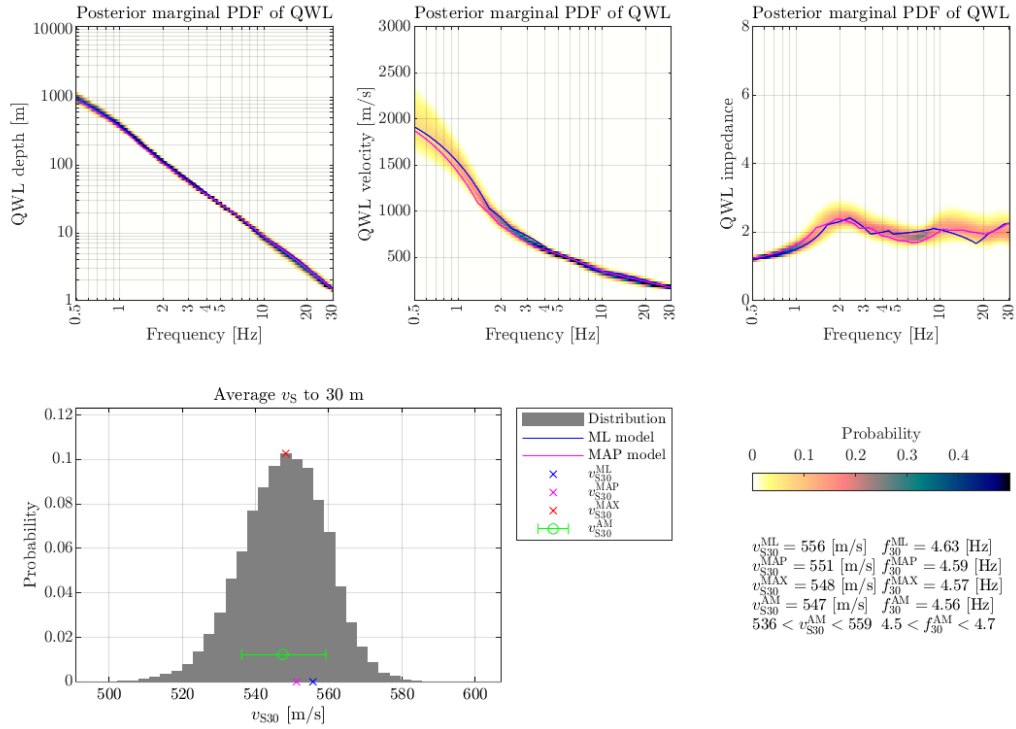
Figure 4: (Top) QWL parameters (depth, velocity, inverse of the impedance contrast; see Poggi et al., 2012) from the inverted Vs profiles. (Bottom) Average Vs30 distribution obtained from the inverted profiles.
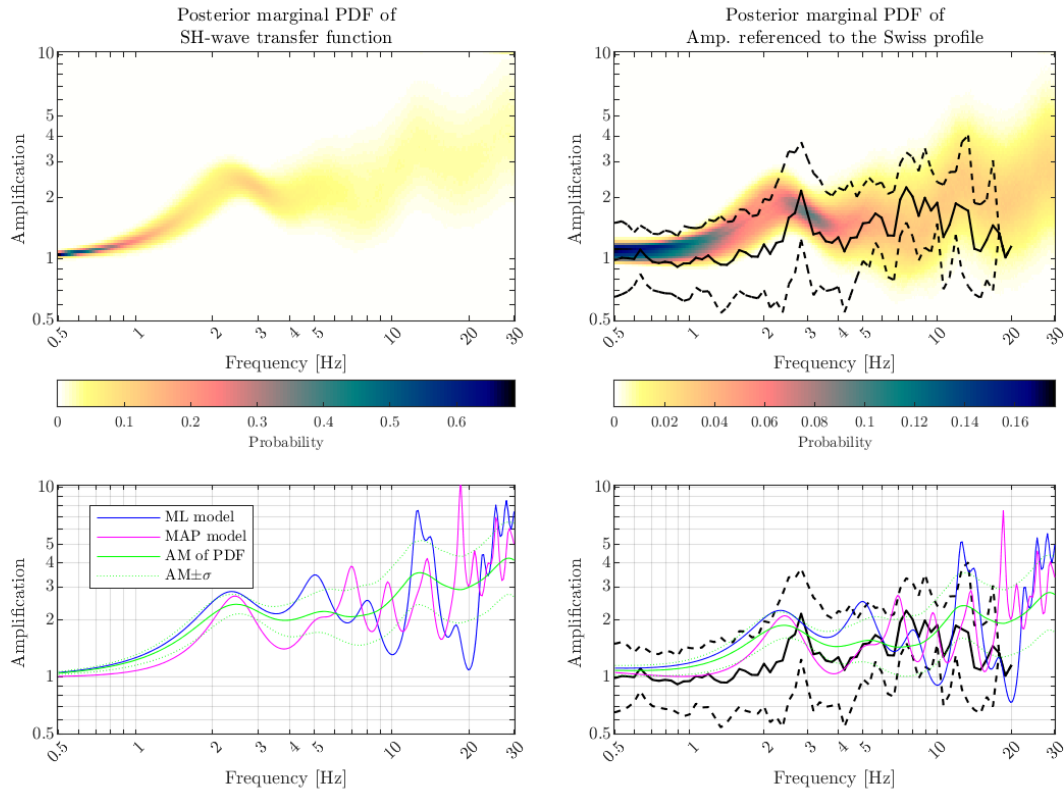

Figure 5: (Top) Posterior marginal PDF on amplification of SH-wave outcrop-surface transfer function in case of unreferenced (left) and referenced (right) to Swiss reference rock model (Poggi et al., 2011). (Bottom) SH-wave transfer functions for the retrieved ML and MAP models for unreferenced and referenced cases. The black curves represent the EAF from the seismic station and its uncertainty (EAF±σ).

References:

Edwards, B., Michel, C., Poggi, V., & Fäh, D. (2013). Determination of Site Amplification from Regional Seismicity: Application to the Swiss National Seismic Networks, Seismol. Res. Lett., 84(4), 2013.

Eurocode 8 (2004). Design of structures for earthquake resistance – Part 1: general rules, seismic actions and rules for buildings. European Committee for Standardization, en 1998-1 edition.

Hallo, M., Imperatori, W., Panzera, F. & Fäh, D. (2021). Joint multizonal transdimensional Bayesian inversion of surface wave dispersion and ellipticity curves for local near-surface imaging. Geophysical Journal International, 266, 627–659.

Hobiger et al. (2021). Site Characterization of Swiss Strong-Motion Stations: The Benefit of Advanced Processing Algorithms. Bulletin of the Seismological Society of America 2021; 111 (4): 1713–1739

Hobiger M., P.-Y. Bard, C. Cornou, and N. Le Bihan (2009). Single station determination of Rayleigh wave ellipticity by using the random decrement technique (RayDec). Geophysical Research Letters, Vol. 36, L14303

Michel, C., Bergamo, P., Hobiger, M., Fäh, D. (2016). Site characterization report SSCN: Schweizerhalle (BL) - Novartis. Internal report, Schweizerischer Erdbebendienst (SED), ETH Zürich.

Poggi, V., Edwards, B. & Fäh, D. (2012). "Characterizing the Vertical-to-Horizontal Ratio of Ground Motion at Soft-Sediment Sites", Bull. Seismol. Soc. Am., 102(6), 2741–2756.

Poggi, V., Edwards, B. & Fäh, D. (2011). Derivation of a Reference Shear-Wave Velocity Model from Empirical Site Amplification, Bull. Seismol. Soc. Am., 101(1), 258–274.

Joyner, W.B., Warrick, R.E. & Fumal, T.E. (1981). "The effect of Quaternary alluvium on strong ground motion in the Coyote Lake, California, earthquake of 1979", Bull. Seismol. Soc. Am., 71(4), 1333–1349.

SIA, Società svizzera degli ingengneri e degli architetti, 2020. SIA 261 - Azioni sulle strutture portanti. Società svizzera degli ingengneri e degli architetti, Zurich, Switzerland.